

The influence of carboxylate ions on the growth of β -FeOOH particles

T. ISHIKAWA, S. KATAOKA, K. KANDORI

School of Chemistry, Osaka University of Education, 4-88 Minamikawahori-cho, Tennoji-ku, Osaka 543, Japan

Colloidal β -FeOOH particles were produced by hydrolysis of FeCl_3 solutions doped with varied amounts of formate, lactate, oxalate, tartarate, pyromellitate and EDTA ions at 100 °C. The resulting particles were characterized by X-ray diffraction, transmission electron microscopy, thermogravimetric-differential thermal analysis, Fourier transform-infrared spectroscopy, elemental analysis, and the adsorption of nitrogen and water. With increasing concentration of added carboxylate ions, the mean modal size of the particles formed increased at low concentrations and decreased after passing the maximum. The crystallite sizes also revealed a maximum on adding EDTA, oxalate and lactate ions, while they monotonically decreased with the addition of other ions. Doping with tartarate and pyromellitate ions by more than 7 and 10 mol%, respectively, produced amorphous particles containing a large amount of these ions. The particles formed with 20 mol% tartarate ions adsorbed water selectively.

1. Introduction

The effects of various organic anions such as carboxylate and hydroxycarboxylate ions on the formation of ferric oxides or oxide hydroxides have so far been a matter of interest in soil science, biology and medical science, because these substances exist in soils and organisms. Nowadays, ferric oxides and oxide hydroxides are raw materials for manufacturing pigments, powders for magnetic memory, catalysts, etc. In these applications, controlling the particle shape, size and crystallinity of the ferric compounds is necessary for producing high-performance products. However, few successful methods have yet been invented; for instance, the preparation of monodispersed α - Fe_2O_3 [1–3], γ - Fe_2O_3 [4] and Fe_3O_4 [5] particles by Matijević and co-workers, because the mechanism of the formation of these materials is still unclear despite extensive studies. When ferric oxide or oxide hydroxide particles are prepared from aqueous ferric solutions, the addition of the anions which strongly interact with Fe^{3+} ions and/or the surface of the resulting nuclei particles, is presumed to be a method available for controlling the structures and properties of the particles produced. Schwertmann and co-workers [6–8] have investigated the influence of various organic and inorganic anions on the formation and crystal growth of α - Fe_2O_3 and α -FeOOH and found that these anions inhibit or retard the crystallization of these oxides. Kodama and Schnitzer [9] studied the inhibitory effect of fulvic acid on the crystallization of α - Fe_2O_3 and α -FeOOH. The effects of carboxylic acids on the crystal growth of α -FeOOH [10] and the formation of γ -FeOOH [11] were also studied. Recently, we have investigated not only the influence of

citrate ions [12], phosphate and silicate ions [13], and amines [14] on the formation of α - and β -FeOOH particles but also the structures and properties of the resulting materials, and discovered several interesting properties of the products; for instance, the selective adsorption of water on the amorphous particles prepared with citrate ions [15]. However, to our knowledge there appears to be no study of the influence of carboxylate ions on the formation and crystallization of β -FeOOH.

This work was designed to investigate the influences of various carboxylate ions on the formation and particle growth of β -FeOOH by characterizing the materials formed using various techniques.

2. Experimental procedure

500 ml 0.1 mol l⁻¹ FeCl_3 solution containing different amounts of carboxylate ions was heated at 100 °C in a capped 1 l Pyrex vessel for 5 h unless otherwise stated. The pH of the suspensions after this ageing were less than 1 at room temperature. The precipitates formed were separated from the solution by centrifuging and thoroughly washed with distilled water and then dried in an air oven at 70 °C. The carboxylate ions added to the starting solutions were formate, oxalate, lactate, *d*, *l*-tartarate, pyromellitate and EDTA ions, the origins of which were respective sodium salts or acids of Wako Reagent grade. The added amounts of these ions were 0–50 mol % to Fe^{3+} ions.

The materials thus prepared were characterized by various means. Powder X-ray diffraction (XRD) was done using a diffractometer with nickel-filtered CuK_α radiation (30 kV, 15 mA). The morphology of the

particles was observed by transmission electron microscopy (TEM). Infrared spectra in KBr were recorded with a Fourier transformation – infrared (FT-IR) spectrophotometer. Simultaneous thermogravimetry and differential thermal analysis (TG-DTA) was performed using a thermoanalyser in air at a heating rate of $5\text{ }^{\circ}\text{C min}^{-1}$. The carbon content in the prepared materials was assayed using a CHN analyser and the iron content was determined by inductively coupled plasma spectroscopy (ICP) by first dissolving in hydrochloric acid. The specific surface area was calculated by applying the BET equation to nitrogen adsorption isotherms at liquid nitrogen temperature recorded by an automatic volumetric apparatus designed in our laboratory. The water adsorption isotherms were measured using a computer-aided automatic gravimetric equipment. Before water and nitrogen adsorption, the samples were treated under 10^{-2} Pa at $75\text{ }^{\circ}\text{C}$ for 2 h.

3. Results

Transmission electron micrographs of the particles formed by ageing for 5 h in the presence of tartarate, oxalate and lactate ions are shown in Figs 1–3, respectively. In the case of tartarate ions (Fig. 1), on increasing the added amount of these ions, the particle sizes increased below 0.5 mol % and then decreased. Above 10 mol %, the amorphous agglomerates of very fine particles were formed. EDTA and pyromellitate ions showed a tendency similar to tartarate ions. As is seen in Fig. 2, the particle sizes increased with increasing amount of oxalate ions, up to 5 mol %, above which the formed particles became aggregated. However, the XRD patterns of the created agglomerates were characteristics of $\beta\text{-FeOOH}$, differing from the case of tartarate ions. As can be seen from Fig. 3, the addition of lactate ions markedly increased the particle sizes below 20 mol %, and gave irregular particles above 30 mol %.

Fig. 4 shows the XRD patterns of the materials formed with various amounts of tartarate ions.

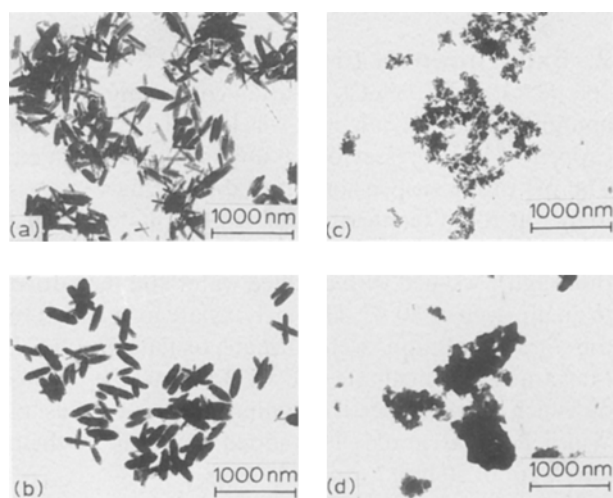


Figure 1 Transmission electron micrographs of the particles formed with various amounts of tartarate ions on ageing for 5 h: (a) 0 mol %, (b) 0.5 mol %, (c) 5.0 mol %, (d) 10.0 mol %.

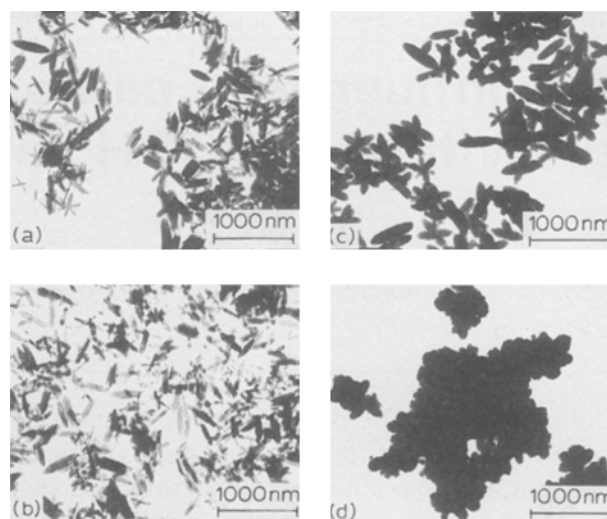


Figure 2 Transmission electron micrographs of the particles formed with different amounts of oxalate ions on ageing for 5 h: (a) 0 mol %, (b) 1.0 mol %, (c) 5.0 mol %, (d) 20.0 mol %.

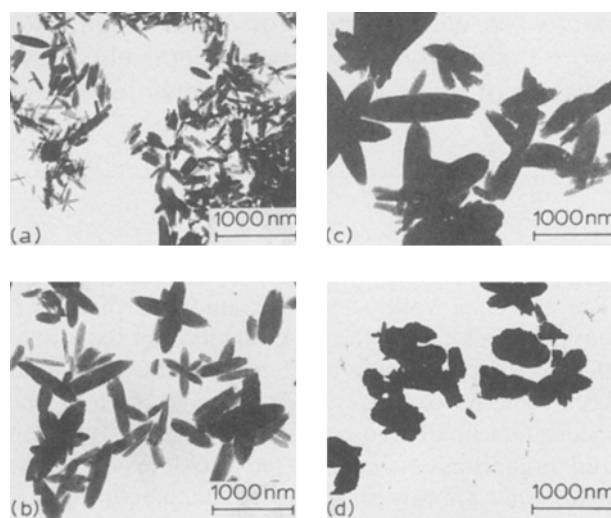


Figure 3 Transmission electron micrographs of the particles formed with various amounts of lactate ions on ageing for 5 h: (a) 0 mol %, (b) 10 mol %, (c) 20 mol %, (d) 30 mol %.

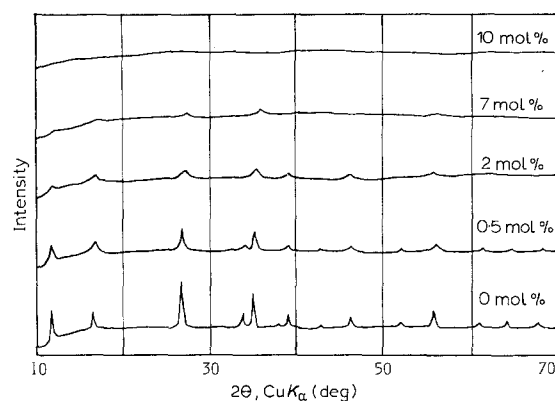


Figure 4 XRD patterns of the materials produced with different amounts of tartarate ions on ageing for 5 h.

Adding these ions lowered the crystallinity of the particles formed until they became amorphous above 10 mol %. On the other hand, the crystallinity of the particles was slightly improved by adding lactate ions,

as can be seen in Fig. 5. The influences of lactate, oxalate and formate ions on the crystallinity of the particles formed were less than those of tartarate, EDTA and pyromellitate ions. Assuming that the broadening of the diffraction peaks reflects only the depression of crystallite size in the particles, the crystallite size can be calculated from a half-width of diffraction peaks using the Scherrer equation. The crystallite size, L , evaluated from the peak due to the reflection from the (200) plane is plotted against the amount of various carboxylate ions in Fig. 6. The L values of the materials formed with EDTA, oxalate and lactate ions, showed a maximum, as seen in Fig. 6. The maximum L values were in the order EDTA > oxalate > lactate ions, and the concentrations of these ions which showed a maximum L value were in the opposite order. At high concentrations, tartarate, EDTA and pyromellitate ions reduced the L values of the products further, compared to the other ions.

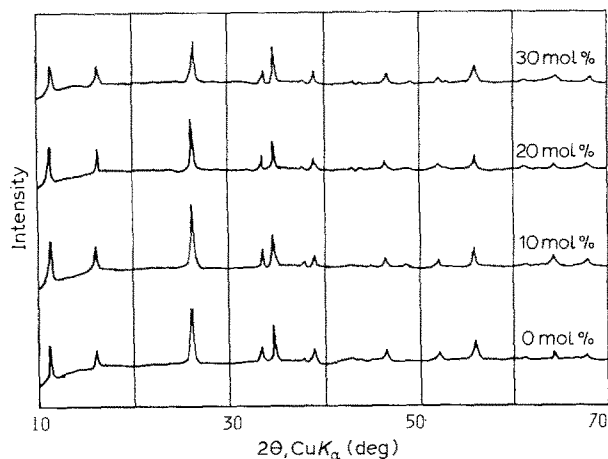


Figure 5 XRD patterns of the materials produced with various amounts of lactate ions on ageing for 5 h.

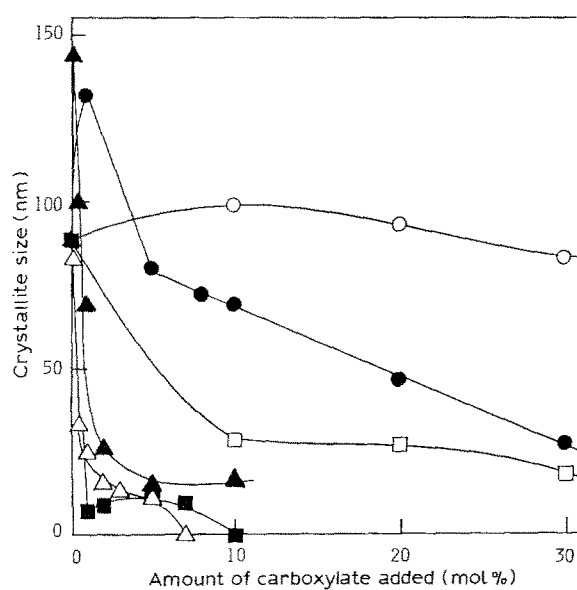


Figure 6 Crystallite sizes, L_{200} , of β -FeOOH of the materials formed with different amounts of various carboxylate ions ageing for 5 h: (○) lactate, (●) oxalate, (□) formate, (▲) EDTA, (△) tartarate, (■) pyromellitate.

Fig. 7 shows infrared spectra of the materials formed with tartarate ions. The spectrum of the material formed without these ions was characteristic of β -FeOOH [16]. The spectra of the materials formed with tartarate ions showed absorption bands due to tartarate ions coordinating to ferric ions, as can be deduced from the spectrum of sodium tartarate shown by the dashed line in Fig. 7. With increasing added amount, the intensity of the bands due to tartarate ions increased and the bands of β -FeOOH diminished. In the cases of carboxylate ions other than tartarate and pyromellitate, the bands of the respective carboxylate ions were very weak and the bands of β -FeOOH appeared even above 10 mol %.

The TG-DTA curves of the materials formed with tartarate ions are shown in Fig. 8. The DTA curve of

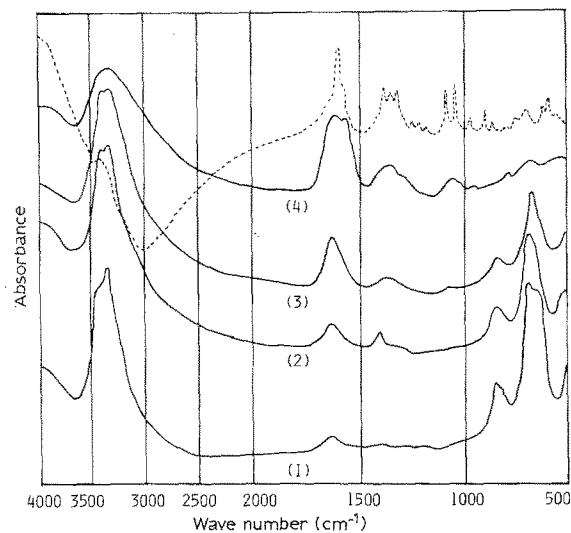


Figure 7 FT-IR spectra of the materials formed with different amounts of tartarate ions on ageing for 5 h: (1) 0 mol %, (2) 1.0 mol %, (3) 5.0 mol %, (4) 10.0 mol %. (---) The spectrum of sodium tartarate.

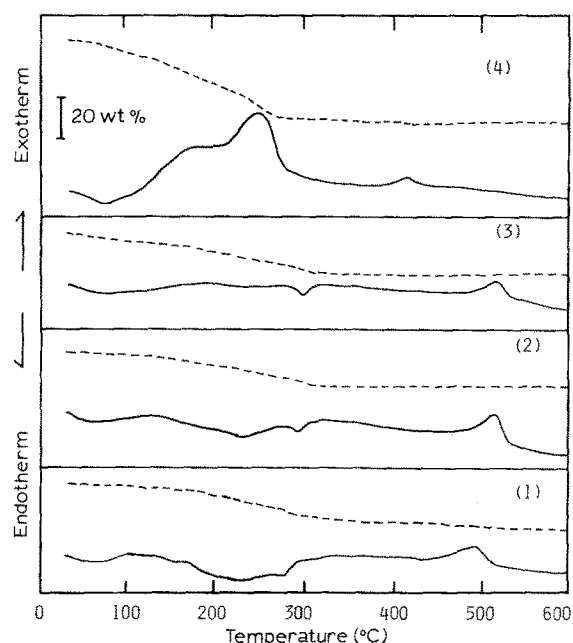


Figure 8 DTA-TG curves of the materials formed with different amounts of tartarate ions on ageing for 5 h: (1) 0 mol %, (2) 0.3 mol %, (3) 3.0 mol %, (4) 10.0 mol %.

the sample prepared without these ions was characteristic of β -FeOOH. The endothermic peak at 240 °C is due to the dehydroxylation of β -FeOOH and the exothermic peak at 495 °C is due to the crystallization from amorphous ferric oxide to α -Fe₂O₃ [16]. The endothermic peak accompanied a weight loss in the TG curve. The small peak at 280 °C resulted from the release of chlorine contained in the β -FeOOH crystals. With increasing concentration of added tartarate ions, the endothermic peak at 240 °C became small and a large exothermic peak appeared around 250 °C, which could be caused by the decomposition and/or oxidation of tartarate ions, because this peak was accompanied by a large weight loss. Pyromellitate ions showed the same tendency as tartarate ions, but lactate ions essentially did not affect the TG-DTA curves.

The results of FT-IR indicate that the materials formed with carboxylate ions, especially tartarate and pyromellitate ions, contain a significant amount of these ions. The contents of residual carboxylate ions, determined by means of the elemental analysis, are plotted in Fig. 9 against the amount of these ions added to the starting solutions. The contents of tartarate and pyromellitate ions were larger than those of the other carboxylate ions, and increased steeply above 7 mol % with the amount added, while those of the other carboxylate ions increased slightly. These results agree well with the results of FT-IR and TG-DTA.

As stated above, ageing for 5 h gave only β -FeOOH particles. However, ageing for more than 48 h yielded a mixture of β -FeOOH and α -Fe₂O₃. Fig. 10 demonstrates the change in L values of β -FeOOH and α -Fe₂O₃ with ageing time as a function of the concentration of added tartarate ions. On extending the ageing time without tartarate ions, the L value of β -FeOOH increased up to 24 h and then decreased. After ageing for 120 h, the XRD peaks of β -FeOOH disappeared. The L value of α -Fe₂O₃ increased following the decrease in the L value of β -FeOOH. On the other hand, in the system with 10 mol % tartarate ions, the L value of β -FeOOH increased with ageing time up to 48 h, and then was almost constant.

The adsorption isotherms of nitrogen and water were measured for the analysis of the surface and pore

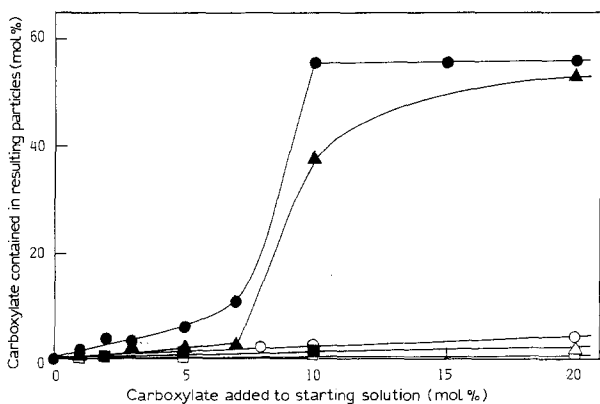


Figure 9 Relations between amounts of carboxylate ions added to the starting solutions and those contained in the resulting materials. The ageing time was 5 h. (●) tartarate, (▲) pyromellitate, (○) oxalate, (△) lactate, (□) formate.

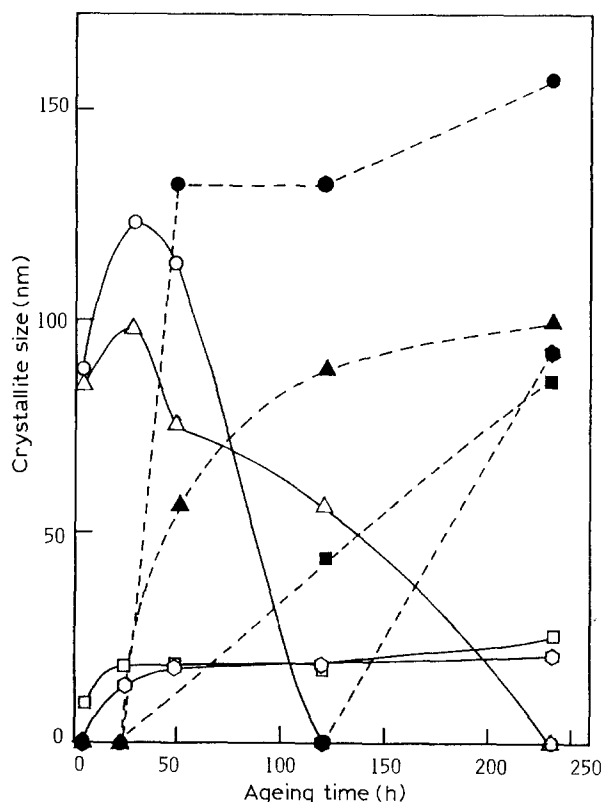


Figure 10 Crystallite sizes, L , of (—) β -FeOOH and (---) α -Fe₂O₃ of the materials formed with different amounts of tartarate ions on ageing for different times. The L values of β -FeOOH and α -Fe₂O₃ were calculated from the diffraction peaks of (200) and (310) planes, respectively. (○, ●) 0 mol %, (△, ▲) 0.1 mol %, (□, ■) 1.0 mol %, (◇, ●) 10.0 mol %.

structures of the particles formed with carboxylate ions. The specific surface areas, S_n , calculated from the nitrogen adsorption isotherms by the BET method are plotted against the concentrations of tartarate, oxalate and pyromellitate ions added to the starting solutions in Fig. 11. The S_n value of the materials formed with

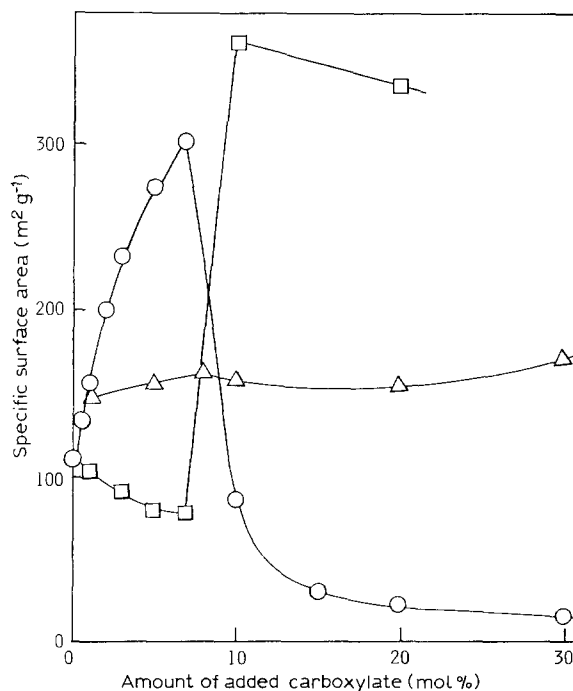


Figure 11 Specific surface areas of the materials formed with different amounts of (○) tartarate, (△) oxalate and (□) pyromellitate ions on ageing for 5 h.

tartarate ions increased steeply with increasing added amount, but above 7 mol % it abruptly decreased, whereas, the S_n value decreased with the addition of pyromellitate ions up to 7 mol %, and above 10 mol % drastically increased. For oxalate ions, the S_n value increased below 1 mol %, but above this concentration remained nearly constant.

Fig. 12 shows the BET monolayer adsorption capacity of water per unit nitrogen surface area, A_m , of the materials produced with varied concentrations of tartarate, oxalate and pyromellitate ions. The materials formed with less than 10 mol % pyromellitate ions showed larger A_m values than those formed with the other ions. In the case of tartarate ions, the A_m value decreased with increasing the concentration up to 7 mol %, and then steeply increased. The A_m values of the materials formed with oxalate and pyromellitate ions were almost constant above 1 and 10 mol %, respectively. The dashed line of this figure indicates the theoretical A_m values of 9.3 molecules nm^{-2} evaluated from a cross-sectional area of H_2O molecules (0.108 nm^2) assuming that the entire surface of the materials is accessible to both water and nitrogen molecules. All of the A_m values given in Fig. 12 are larger than this theoretical value. It is especially of interest that the A_m value of the material produced with 20 mol % tartarate ions is extremely large.

4. Discussion

4.1. Effects of carboxylate ions

The carboxylate ions influenced the crystal growth of $\beta\text{-FeOOH}$ in different ways, as can be seen from Fig. 6. It can be generally considered that inorganic or organic anions affect the formation of metal oxide or hydroxides through the following processes: (1) the chelating of these ions with metal ions to prevent the hydrolysis of metal ions, i.e. nucleation; (2) the adsorption of these ions on the nuclei produced by hydrolysis

to inhibit the growth of the nuclei [8, 17]. The maximum crystallite and particle size observed for the system with added EDTA, oxalate and lactate ions in Fig. 6 can be interpreted by the following mechanism. The hydrolysis of Fe^{3+} ions is inhibited, in part, by the addition of these carboxylate ions so that only a few nuclei are formed. This leads to the formation of larger particles, because after nucleation the number of the particles does not increase but only particle growth takes place. On the other hand, carboxylate ions adsorb on the resulting nuclei to interfere with their growth. Therefore, the appearance of the maximum is thought to relate to the balance between the degrees of adsorption and complexation. The adsorption and complexation abilities of carboxylate ions depend upon their structures, especially the number of OH and COO^- groups. It is clear from Fig. 6 that EDTA, pyromellitate and tartarate ions more markedly decreased the crystallite size of $\beta\text{-FeOOH}$ compared to lactate, oxalate and formate ions possessing fewer COO^- and OH^- groups, except for a low concentration region showing a maximum. The former three ions may more strongly and effectively adsorb on the nuclei or particles than the latter three, because a larger ion with more functional groups can occupy more strongly a wider area of the particle surface. This can also be used to explain the results of Fig. 6: the concentration of carboxylate ions showing maximum L values was in the order EDTA > oxalate > lactate ions, while the height of the maxima was in the opposite order. That is, EDTA ions having a higher ability to be adsorbed and to undergo complexation, show a larger maximum L value at a lower concentration. However, no maximum appeared for pyromellitate and tartarate ions, although the strong adsorption and complexation of these ions can be speculated from the results of TG-DTA, FT-IR and elemental analysis. This conflict may be because the concentrations of these ions showing the maximum L value are too low to be detected in the present experiments.

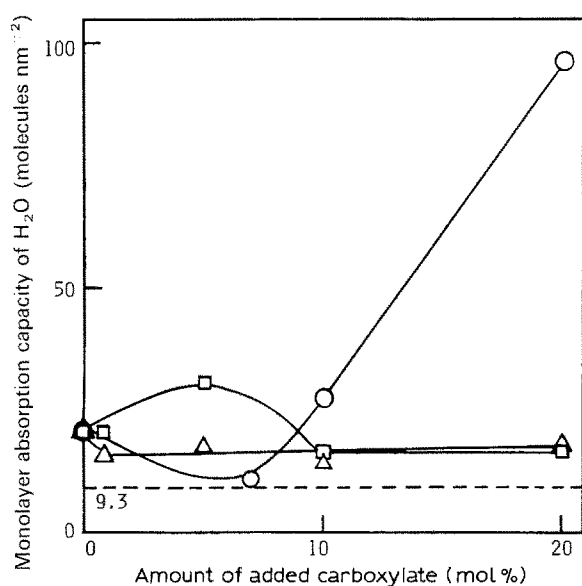


Figure 12 Water monolayer adsorption capacity per nitrogen surface area of the materials formed with various amounts of (○) tartarate, (△) oxalate and (□) pyromellitate ions on ageing for 5 h.

4.2. Structures of the particles formed

A further understanding of the role of carboxylate ions requires structural analysis of the materials formed. In a previous work we found that the amorphous particles formed with citrate ions adsorb H_2O molecules selectively [15]. Fig. 12 indicates that all the materials adsorb water molecules more than nitrogen molecules even for the pure $\beta\text{-FeOOH}$, because the A_m values are larger than 9.3 molecules nm^{-2} . This selective adsorption of water is considered to be due to the tunnels in the $\beta\text{-FeOOH}$ crystals which are accessible to water molecules but not to nitrogen molecules [18]. Therefore, the decrease in the A_m values on addition of these three ions seems to be caused by rupture of the tunnel structure. In particular, the materials formed with more than 10 mol % tartarate ions showed a large A_m value, that is, a high selective adsorption of water. The particles produced with pyromellitate ions showed a maximum of A_m at ~ 5 mol %, though the particles formed with tartarate ions showed a minimum.

Cornell and Schwertmann [8] thought that the crystallization of $\alpha\text{-Fe}_2\text{O}_3$ was inhibited by tartaric acid linking ferric hydroxide particles of 2–4 nm diameter. An analogous mechanism might be applied to the inhibition of crystallization of $\beta\text{-FeOOH}$ by adding carboxylate ions, with the exception of formate and lactate ions which are incapable of linking as speculated from their molecular structures. As seen in Figs 1 and 11, the large irregular particles of low S_n values were produced on adding more than 10 mol % tartarate ions. These particles appear to be agglomerates of small particles between which the ultramicropores accessible to water molecules, but not to nitrogen molecules, are formed. On the contrary, the amorphous particles produced by adding more than 10 mol % pyromellitate ions had a high surface area and a low A_m value. The opposite results for these two ions would be associated with the difference in their molecular structures; pyromellitate ions, having phenyl groups, are much larger in comparison with tartarate ion. Therefore, the micropores in the particles formed with the pyromellitate ions are large enough to be accessible to both water and nitrogen molecules, so these particles showed a higher S_n value and a smaller A_m value than the particles formed with tartarate ions. Such a microporosity of the particles with pyromellitate ions is obvious from the nitrogen adsorption isotherms, rising steeply in low relative pressures. These findings suggest that the porosity of ferric oxides can be controlled using the correct carboxylate ion.

4.3. Transformation of $\beta\text{-FeOOH}$ to $\alpha\text{-Fe}_2\text{O}_3$

It is well known that $\beta\text{-FeOOH}$ transforms to $\alpha\text{-Fe}_2\text{O}_3$ in an acidic solution under various conditions. We found recently, that citrate ions affect this phase transformation. As details of the results will be soon reported elsewhere, the present paper describes only the influence of tartarate ions. It is clear from Fig. 10 that tartarate ions inhibit the conversion of $\beta\text{-FeOOH}$ to $\alpha\text{-Fe}_2\text{O}_3$. The mechanism of the transformation of $\beta\text{-FeOOH}$ to $\alpha\text{-Fe}_2\text{O}_3$ in aqueous media is thought to be dissolution of $\beta\text{-FeOOH}$ and recrystallization to $\alpha\text{-Fe}_2\text{O}_3$. In the case of tartarate ions, the less-crystalline $\beta\text{-FeOOH}$ phase remained even at 10 mol % after 240 h ageing, as can be seen from the solid lines of Fig. 10, indicating that dissolution of $\beta\text{-FeOOH}$ is disrupted by these ions. On the other hand, the crystallization of $\alpha\text{-Fe}_2\text{O}_3$ was also retarded by tartarate

ions, as shown by the dashed lines in the same figure. Such inhibitory effects of tartarate ions on dissolution of $\beta\text{-FeOOH}$ and recrystallization of $\alpha\text{-Fe}_2\text{O}_3$ could be explained in terms of complexation and adsorption in a similar manner to the formation and growth of $\beta\text{-FeOOH}$ particles described above.

Acknowledgements

We thank Dr Yoshihira Okanda and Dr Masao Fukusumi, Osaka Municipal Technical Research Institute, for their help in the TEM measurements. This research was supported in part by the Science Research Fund of the Ministry of Education of Japanese Government.

References

1. E. MATIJEVIĆ and P. SCHEINER, *J. Colloid Interface Sci.* **63** (1978) 509.
2. N. KALLAY, I. FISCHER and E. MATIJEVIĆ, *Colloids Surfaces* **13** (1985) 145.
3. M. OZAKI, S. KRATOHVIL and E. MATIJEVIĆ, *J. Colloid Interface Sci.* **102** (1984) 146.
4. M. OZAKI, and E. MATIJEVIĆ, *ibid.* **107** (1985) 199.
5. R. S. SAPIESZKO and E. MATIJEVIĆ, *ibid.* **74** (1980) 405.
6. U. SCHWERTMANN, *Nature* **212** (1966) 645.
7. *Idem*, *Geoderma* **3** (1969) 207.
8. R. M. CORNELL and U. SCHWERTMANN, *Clays Clay Mineral.* **27** (1979) 402.
9. H. KODAMA and M. SCHNITZER, *Geoderma* **19** (1977) 279.
10. T. F. BARTON, T. PRICE, K. BECKER and J. G. DILLARD, *Colloids Surfaces* **53** (1991) 209.
11. T. F. BARTON, T. PRICE and J. G. DILLARD, *J. Colloid Interface Sci.* **138** (1990) 122.
12. K. KANDORI, M. FUKUOKA and T. ISHIKAWA, *J. Mater. Sci.* **26** (1991) 3313.
13. K. KANDORI, S. UCHIDA, S. KATAOKA and T. ISHIKAWA, *J. Mater. Sci.*, **27** (1992) 719.
14. T. ISHIKAWA, T. TAKEDA and K. KANDORI, *ibid.* **27** (1992) 4531.
15. K. KANDORI and T. ISHIKAWA, *Langmuir*, **7** (1991) 2213.
16. T. ISHIKAWA and K. INOUYE *Bull. Chem. Soc. Jpn* **48** (1975) 1580.
17. R. M. CORNELL and P. W. SCHINDLER, *Colloid Polym. Sci.* **258** (1980) 1171.
18. T. ISHIKAWA and K. INOUYE, *Bull. Chem. Soc. Jpn* **46** (1973) 2665.
19. R. J. ATKINSON, A. M. POSNER and J. P. QUIRK, *Clays Clay Mineral.* **25** (1977) 49.

Received 24 October 1991
and accepted 14 August 1992